ELSEVIER

Catalysis Today 69 (2001) 51–55

CATALYSIS TODAY

www.elsevier.com/locate/cattod

Gas–liquid mass transfer of aqueous Taylor flow in monoliths

Johan J. Heiszwolf, Michiel T. Kreutzer, Menno G. van den Eijnden, Freek Kapteijn*, Jacob A. Moulijn

Section Industrial Catalysis, Delft ChemTech, Delft University of Technology, Julianalaan 136, 2628 BL Delft, The Netherlands

Abstract

The gas–liquid mass transfer of a monolith operating in the Taylor flow regime is presented. Mass transfer measurements are compared with a literature model derived for single capillaries. The comparison resulted in a prediction of the unit cell length (gas bubble + liquid slug). Independent measurements of the liquid slug length showed that the predicted unit cell length is close to the measured ones. This leads to the conclusion that mass transfer models for single capillaries may indeed be used for monoliths. Additionally, it is shown that the liquid slug length may also be estimated from pressure drop measurements.

Keywords: Gas–liquid mass transfer; Taylor flow; Unit cell length; Liquid slug length; Monolith

1. Introduction

The monolith is a type of structured packing that is widely used for solid-catalyzed gas-phase chemical reactions, i.e. in many power plants the flue gas is treated with monolithic units to remove NO_x and in the western world each new car that runs on petrol is equipped with a monolithic three-way catalyst. One may conclude that for gas–solid reaction systems, the monolith is proven technology. Application of monolith reactors for gas–liquid–solid applications is relatively new [1]. At present, one type of commercial monolith reactor is operational at five different plants of AKZO-Nobel [2,3]. However, a substantial amount of chemical and biological catalyzed gas–liquid reactions have been carried out in bench-scale monolith reactors [4,5] and also in the chemical industry an increasing interest in application of monoliths for three-phase reaction systems can be perceived [6,7].

Fig. 1 shows a possible configuration of a monolith reactor system for three-phase applications. It consists of a monolith section, a gas–liquid separator, a pump and a heat exchanger. The gas flow can be circulated using the suction created by the liquid flow or can be forced through the monolith with an additional gas compressor. Because the pressure drop across a monolith is very low, the liquid can be circulated at relatively high flow rates without the need of a special pump. Note that in contrast to a Buss loop reactor, the liquid does not contain catalyst particles which makes the design of the pump and heat exchanger straightforward. One of the advantages of this so-called *monolith loop reactor* is that the mass transfer and the heat transfer zones are separated and can be scaled independently. This degree of freedom in design is not present for conventional three-phase reactors like the trickle bed or the slurry stirred tank reactor. Benefits of the monolithic catalyst are the short internal diffusion lengths due to the thin catalyst layer (less than

Abbreviations: cpsi, cells per square inch

*Corresponding author. Fax: +31-15-278-4452.
E-mail address: f.kapteijn@stm.tudelft.nl (F. Kapteijn).

0920-5861/01/$ – see front matter
PII: S0920-5861(01)00354-6

Nomenclature

d_b	bubble diameter (m)
d_c	channel diameter (m)
D	diffusion coefficient (m^2/s)
f	friction factor (–)
k_La	gas–liquid mass transfer parameter (s^{-1})
L_S	liquid slug length (m)
L_U	unit cell length (m)
Re	Reynolds number (–)
u_G	gas velocity (m/s)
u_L	liquid velocity (m/s)
u_{UC}	two-phase velocity, $u_{UC} = u_G + u_L$ (m/s)

Greek symbols

ε_L	liquid hold-up (–)
Ψ_S	liquid slug length, $\Psi_S = L_S/d_c$ (–)
Ψ_{UC}	unit cell length, $\Psi_{UC} = L_{UC}/d_c$ (–)

20 μm) and the high external mass transfer values due to the bubble train flow inside the channels.

To design a monolith reactor, correlations for hold-up, pressure drop, residence time and mass transfer coefficients, are required. These key parameters are studied in our institute. In this paper, the gas–liquid mass transfer parameter k_La is measured using oxygen absorption in water. Additionally, the length of the liquid slugs of the bubble train flow is measured using platinum microprobes inserted into the monolith channels.

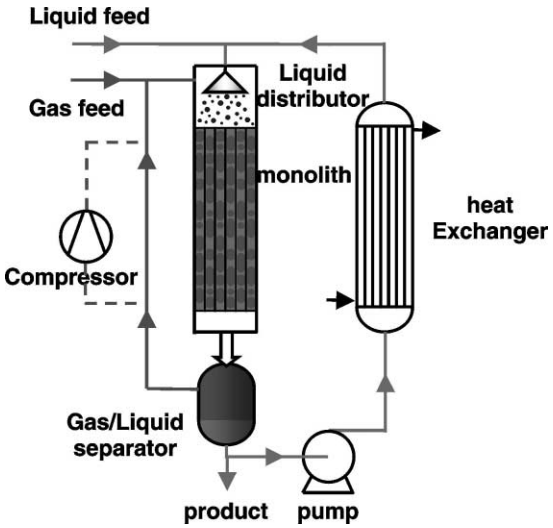

Fig. 1. Schematic diagram of a monolith loop reactor.

2. Theory

If both gas and liquid flow downwards in a small diameter channel, a number of different flow regimes can occur (see Fig. 2). Among these regimes, the important ones are: *annular flow* in which the liquid flows as a film along the wall and gas is transported in the central core, *slug flow* in which the waves of the liquid film occasionally block the channel, *Taylor flow* or *bubble train flow* in which the channel is intermittently filled with gas bubbles and liquid plugs and *dispersed bubble flow* in which the diameter of the bubbles is substantially smaller than that of the tube. Because of the capillary forces, slugging of the channel due to the formation of liquid bridges occurs at even low liquid loading. Moreover, because of the small ($0.5 < d_c/\text{mm} < 5$) monolith channels, dispersed bubble flow ($d_b \ll d_c$) is not likely to occur. As a result of these phenomena, Taylor flow can be obtained in a monolith over a wide range of operating conditions.

In Taylor flow, the gas bubbles have a diameter nearly equal to that of the channel leaving only a thin liquid film between the bubble and the wall. Because the gas bubbles almost block the channels, the liquid flow between two consecutive liquid slugs may be neglected. Due to the stationary wall, a circulating flow is induced in a moving liquid slug. This circulation flow refreshes the gas–liquid interface of the gas bubble continuously, leading to a high gas–liquid mass transfer rate. For a given liquid hold-up, Taylor flow with short liquid slugs will have a higher mass transfer rate than flow in which larger liquid slugs occurs. This is caused by the increased interfacial area and the more intense mixing for short liquid slugs. Note that because of the small channel diameter of monoliths, the flow in the channel remains laminar.

Literature models that predict the transport properties of two-phase flow in monoliths often depend on the values of the liquid slug length or the length of the unit cell (one liquid slug plus one gas bubble), e.g.

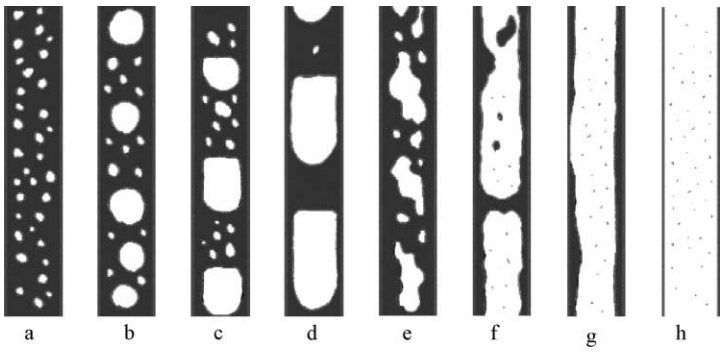

Fig. 2. Different types of two-phase flow in a channel: (a) dispersed bubble flow; (b) bubble flow; (c) elongated bubble flow; (d) Taylor flow; (e) churn flow; (f) slugging flow; (g) annular flow; (h) mist flow.

[8,9]. Drawback of these models for reactor design is that the liquid slug length is not a priori known.

Based on absorption experiments using methane and water, Bercic and Pintar [8] measured the gas to liquid mass transfer parameter $k_L a$ in single capillary tubes of different diameter. They fitted the experimental results to the following empirical correlation:

$$k_L a = \frac{0.133 u_{UC}^{1.2}}{\sqrt{L_s}} \quad (1)$$

in which L_S is the length of the liquid slug and $k_L a$ is based on channel volume. Eq. (1) shows that the mass transfer parameter $k_L a$ increases with decreasing liquid slug lengths and increases with the velocity of the unit cell.

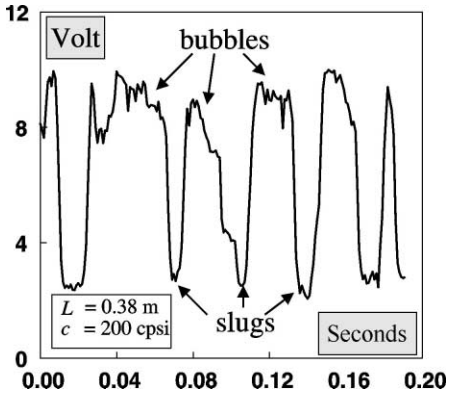

Fig. 3. Typical signal of the conductivity probe, voltage versus time.

3. Experimental

The gas–liquid mass transfer parameter was measured using oxygen absorption [10]. In order to measure the steady-state mass transfer, the gas–liquid separator of Fig. 1 was sparged with nitrogen and air was fed to the monolith section. The oxygen content of the liquid entering and leaving the monolith was measured using two WTW CellOx oxygen probes. To eliminate the mass transfer contribution in the liquid distribution section, monoliths of different lengths were measured. The reported $k_L a$ values in this paper are valid for the flow inside the monolith channel and do not include the contribution of the liquid distributor.

The liquid slug and bubble lengths inside a 200 cpsi monolith have been measured by inserting small platinum micro-probes inside one of the channels ($d_c = 1.56 \times 10^{-3}$ m). One probe is located at the wall of the channel and the other probe, of which only the tip is conductive, is placed in the center of the channel. Across the probes, an alternating current is applied and the voltage difference is measured with a sample frequency up to 10 000 Hz. Fig. 3 shows a typical measured signal in which the gas bubbles and the liquid plugs can be clearly identified. The experiments were carried out using air and water.

4. Results

Fig. 4 shows measured $k_L a$ values as a function of the unit cell velocity for a 200 cpsi monolith ($d_c = 1.56 \times 10^{-3}$ m). Mass transfer increases with

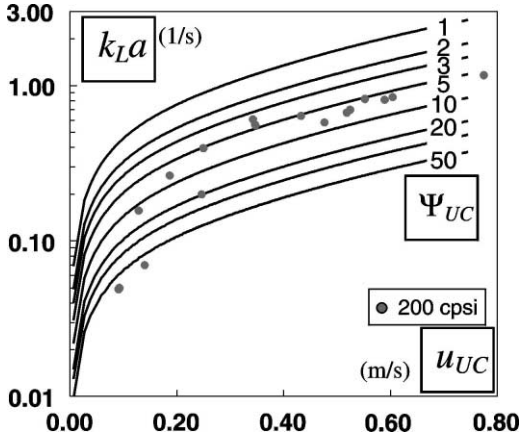

Fig. 4. Gas–liquid mass transfer parameter k_La as a function of the two-phase velocity u_{UC} with the dimensionless slug length Ψ_{UC} as parameter. The lines were calculated with Eqs. (1) and (2).

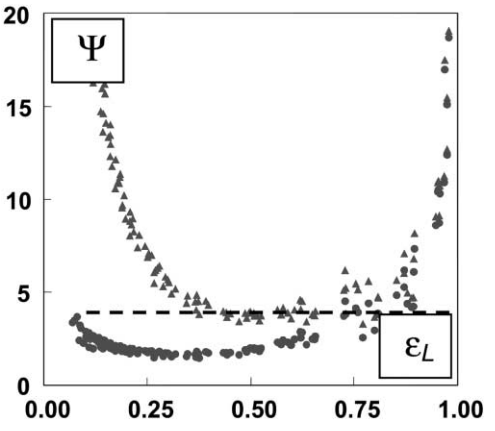

Fig. 5. Measured liquid slug length Ψ_S (circles) and unit cell length Ψ_{UC} (triangles) from Eq. (3) as a function of the liquid hold-up. The dashed line indicates $\Psi_{UC} = 4$.

increasing unit cell velocities. Using the relationship $L_S = \varepsilon_L L_{UC}$ and Eq. (1), a series of model predictions were calculated for different values of the unit cell length Ψ_{UC}. From Eq. (1), which is valid for methane/water, predictions for the oxygen/water system were obtained from

$$k_La|_{O_2} = k_La|_{CH_4} \left[\frac{\mathbf{D}_{O_2}}{\mathbf{D}_{CH_4}} \right]^{\alpha} \quad (2)$$

in which $0.5 < \alpha < 1$, depending on the flow conditions. Since the dependency of the Sherwood number on the Schmidt number is not known for this system, $\alpha = 1$ is used for simplicity. Comparing the experiments with the model predictions, it is clear that for a unit cell length Ψ_{UC} of about 5, a reasonable agreement is obtained. Only at low velocities, the experiments deviate from the model predictions. At these low velocities, an even radial distribution of the liquid across the monolith section could not be obtained. It is further obvious from Fig. 4 that k_La values in the range 0.4–1 s^{-1} can easily be achieved in the monolith. Compared to stirred tanks and trickle beds, these mass transfer values are rather high.

Fig. 5 shows the averaged dimensionless liquid slug length Ψ_S as a function of the liquid hold-up ε_L measured at four different liquid velocities and for a series of gas velocities. The reported slug lengths are the averaged values from 50 to 200 slug length measurements. From this figure, it is clear that the liquid slug length, for this type of monolith, working fluids and liquid distributing system, is a function of the hold-up only and does not additionally depend on the gas or liquid velocities. At high ε_L values, Ψ_S increases sharply because the channel is mostly filled with the liquid phase. It is worth mentioning that at these high hold-up values, the standard deviation of the averaged slug length also increases. In the range $0.25 < \varepsilon_L < 0.5$, the liquid slug length appears to level out at $\Psi_S \approx 2$.

Fig. 5 also shows the unit cell length calculated from the measured liquid slug length:

$$\Psi_{UC} = \frac{\Psi_S}{\varepsilon_L} \quad (3)$$

The unit cell length shows a sharp increase at low liquid hold-up because in this area the unit cell consists of large bubbles. The liquid slug length remains, however, more or less constant. At high liquid hold-up, the unit cell consists of large liquid slugs so that the unit cell length also increases and its values become similar to those of the liquid slug length. In the liquid hold-up range $0.4 < \varepsilon_L < 0.85$, the unit cell length appears to be more or less constant and is approximately $\Psi_{UC} = 4$, as is indicated by the dashed line in Fig. 5. This value is very close to the unit cell length derived from the mass transfer experiments and the model predictions of Eqs. (1) and (2).

For monoliths operating with other phases than air and water, e.g. organic liquids at reaction conditions,

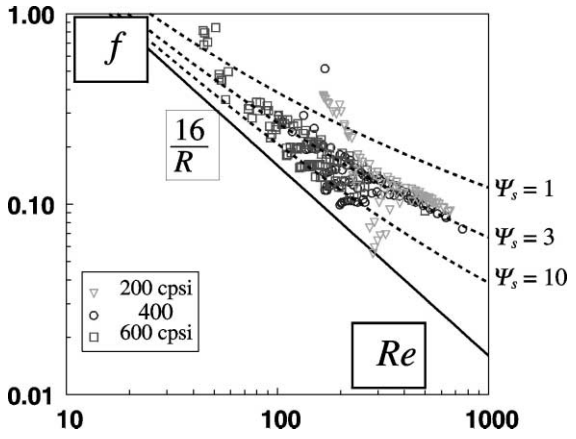

Fig. 6. Experimental two-phase friction-factor f as a function of the Reynolds number Re. The lines correspond to a friction model that depends on the length of the liquid slug Ψ_S.

it may be difficult to measure the liquid slug length. Recently, the two-phase pressure drop has been correlated using a friction-factor model that depends on the liquid slug length [11]. Fig. 6 shows the measured two-phase friction factor as a function of the Reynolds number and three lines representing the friction-factor model for three values of the liquid slug length $\Psi_S = 1$, 3 and 10. This figure shows that the liquid slug length derived from the pressure drop measurements can be estimated close to 3, which is in reasonable agreement with the directly measured slug length. This shows that from relatively easy to carry out pressure drop experiments the liquid slug length can be estimated.

5. Conclusions

Liquid slug lengths and gas–liquid mass transfer for air and water have been measured in monoliths. From the gas–liquid mass transfer measurements and model predictions of Bercic and Pintar [8], a constant unit cell length of $\Psi_{UC} \approx 5$ was predicted. Independent measurements of the liquid slug length using a micro-conductivity probe showed that in the liquid hold-up range $0.4 < \varepsilon_L < 0.85$, a length of $\Psi_{UC} \approx 4$ existed. This result is close to the value that was derived from the mass transfer experiments. We may conclude that the model of Bercic and Pintar [8], Eq. (1), which was derived from experiments in a single capillary tube may also be applied to two-phase flow in a monolith. It is evident that once the liquid slug length is known, the gas–liquid mass transfer of a monolith reactor can be predicted. For reaction systems with physical properties different from water, the liquid slug length may be estimated from easy to carry out pressure drop measurements.

References

[1] F. Kapteijn, J.J. Heiszwolf, T.A. Nijhuis, J.A. Moulijn, Cattech 3 (1999) 24–41.
[2] E. Bengtsson, EP 384,905 AI (1990).
[3] Th. Berglin, W. Herrmann, EP 102,934 A1 (1984).
[4] H.A. Smits, A. Stankiewicz, W.C. Glasz, T.H.A. Fogl, J.A. Moulijn, Chem. Eng. Sci. 51 (1996) 3019–3025.
[5] K.K. Kawakami, K. Kawasaki, F. Shiraishi, K. Kusunoki, Ind. Eng. Chem. Res. 28 (1989) 394–400.
[6] R.M. Machado, D.J. Parrillo, R.P. Boehme, R.R. Broekhuis, US 6,005,143 (1999).
[7] D. Schanke, E. Bergene, A. Holmen, WO98/38147 (1998).
[8] G. Bercic, A. Pintar, Chem. Eng. Sci. 52 (1997) 3709–3719.
[9] V. Hatziantoniou, B. Andersson, Ind. Eng. Chem. Fundam. 21 (1982) 451–456.
[10] J.J. Heiszwolf, L.B. Engelvaart, M.G. van den Einden, M.T. Kreutzer, F. Kapteijn, J.A. Moulijn, Chem. Eng. Sci. 56 (2001) 805–812.
[11] J.J. Heiszwolf, M.G. van der Eijnden, F. Kapteijn, J.A. Moulijn, Int. J. Multiphase Flow, in preparation.